 FDMP, vol.11, no.2, pp.157-170, 2015

Three-dimensional Numerical Study of the Effect of Heating Sources Dimension on Natural Convection in a Cavity Submitted to Constant Heat Flux

L. Belarche[1,2], B. Abourida[1] and S. Smolen[3]

Abstract: Natural convection in a cubical cavity, discretely heated is studied numerically using a three-dimensional finite volume formulation. Two heating square portions are placed on the vertical wall of the enclosure, while the rest of the considered wall is adiabatic. The opposite vertical wall is maintained at a cold uniform temperature and the other walls are adiabatic. Effects of the heating sections dimensions ε ($0.15 \leq \varepsilon \leq 0.35$) and the Rayleigh number Ra ($10^3 \leq Ra \leq 10^7$) on the fluid flow and the heat transfer within the cavity are studied. The obtained results show that the flow intensity and the heat transfer can be significantly improved by an optimal choice of the governing parameters. Streamlines, isotherms and variations of the average Nusselt number are shown for different sets of the considered parameters.

Keywords: Three dimensional natural convection, heated sections dimension, constant heat flux

Nomenclature

Ax	aspect ratio, (L/H)
B	depth of the cavity, (m)
D	height of the square hot section, (m)
g	gravitational acceleration, (m/s^2)
H	height of the cavity, (m)
k	thermal conductivity, (W/m.K)
L	cavity length, (m)
Nu	total average Nusselt number
Pr	Prandtl number, (v/α)
p	non-dimensional pression

[1] National School of Applied Sciences, Ibnou Zohr University, Agadir, Morocco.
[2] Corresponding Author: belarchelahoucine@gmail.com
[3] JRM Institut für Energietechnik der Hochschule, Bremen, Germany.

P	pression, (N/m^2)
q''	heat flux density, (W/m^2)
Ra	Rayleigh number, $(g\beta q'' H^4/\nu\alpha k)$
u,v,w	dimensional velocities, (m/s)
U,V,W	dimensionless velocities
x,y,z	dimensional coordinates, (m)
X,Y,Z	dimensionless cartesian coordinates

Greek symbols

α	thermal diffusivity, (m^2/s)
θ	non-dimensional temperature
β	volumetric thermal expansion coefficient, (K^{-1})
ε	non-dimensional side of the square hot section, (D/H)
μ	dynamique viscosity, (kg/m.s)
ν	kinematic viscosity, (m^2/s)
ρ	density, (kg/m^3)

Subscripts

max	maximum value
c	cold
1	section 1
2	section 2

1 Introduction

The problem of electronic components cooling is often encountered in practical devices. In fact, in thermal control of electronic systems, a careful attention is necessary to ensure an optimal evacuation of the heat surplus. Natural convection represents a simple and low cost mode of cooling, especially for low gradients temperature. Besides this application, natural convection process is also encountered in many practical cases, like solar collectors, buildings design, radiators.... Hence, the problem of natural convective heat transfer in enclosures has been studied extensively. A comprehensive review of this topic is given by Bejan and Kraus (2003) and Goldstein (2006) for different combinations of geometrical and thermal imposed conditions. However, in most of these works, the studied configurations are two dimensional cavities, partially heated, with one or more heating portions [Sharif and Mohammad (2005); Ben Cheikh, Ben Beya and Lili (2007ref$_1$)]. Few works has considered the three-dimensional natural convection [Fusegi, Hyun, Kuwahara and Farouk (1991); Seza and Mohamad (2000); Frederick and Quiroz (2001); Ben-Cheikh, Campo, Ouertatani and Lili (2010)] which gives a more realistic presentation of the fluid motion and the heat exchange within the cavity. In addition, the considered thermal boundary conditions are generally constant heating

temperature. However, the case of imposed heat flux, which is frequently encountered in practical devices, has been considered by very few studies [Ben Cheikh, Ben Beya and Lili (2007ref$_2$); Belarche, Abourida, Smolen and Mediouni (2014)]

Hence, the purpose of the present investigation is to study numerically the fluid flow and heat transfer induced by two heat sources embedded on the left vertical wall of a cubical cavity and submitted to constant heat flux density q''. The rest of the considered wall is adiabatic while the temperature of the opposite vertical wall is maintained at a uniform lower temperature T_c. The governing parameters are the Rayleigh number Ra ($10^3 \leq \text{Ra} \leq 10^7$) and the heating sections dimension $\varepsilon = D/H$ ($0.15 \leq \varepsilon \leq 0.35$). The Prandtl number and the aspect ratio $Ax = L/H$ are fixed respectively to 0.71 and 1.

2 Problem formulation

The schematic configuration of the considered three-dimensional cubical cavity, coordinates and boundary conditions are shown in Fig. 1. Two heat sources are integrated on the left vertical wall of the cavity and submitted to constant heat flux density q''. The rest of the considered wall is adiabatic while the temperature of the opposite vertical wall is maintained at a uniform lower temperature T_c. The other walls are adiabatic. The considered fluid is incompressible, steady-state, Newtonian and verifying the Boussinesq approximation.

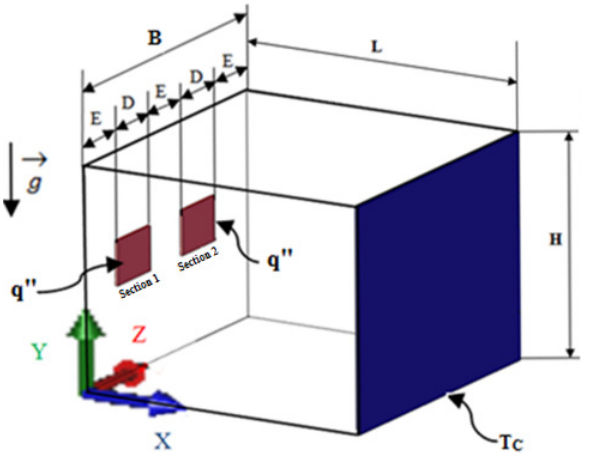

Figure 1: Studied configuration and coordinates

The governing equations for laminar steady convection, using the Boussinesq approximation and neglecting the viscous dissipation, are expressed in the following

dimensionless form:

$$\frac{\partial U}{\partial X}+\frac{\partial V}{\partial Y}+\frac{\partial W}{\partial Z}=0 \tag{1}$$

$$\frac{\partial U}{\partial \tau}+\frac{\partial}{\partial X}(UU)+\frac{\partial}{\partial Y}(VU)+\frac{\partial}{\partial Z}(WU)=-\frac{\partial P}{\partial X}+\Pr(\frac{\partial^2 U}{\partial X^2}+\frac{\partial^2 U}{\partial Y^2}+\frac{\partial^2 U}{\partial Z^2}) \tag{2}$$

$$\frac{\partial V}{\partial \tau}+\frac{\partial}{\partial X}(UV)+\frac{\partial}{\partial Y}(VV)+\frac{\partial}{\partial Z}(WV)=-\frac{\partial P}{\partial Y}+Ra\Pr\theta + \Pr(\frac{\partial^2 V}{\partial X^2}+\frac{\partial^2 V}{\partial Y^2}+\frac{\partial^2 V}{\partial Z^2}) \tag{3}$$

$$\frac{\partial W}{\partial \tau}+\frac{\partial}{\partial X}(UW)+\frac{\partial}{\partial Y}(VW)+\frac{\partial}{\partial Z}(WW)=-\frac{\partial P}{\partial Z}+\Pr(\frac{\partial^2 W}{\partial X^2}+\frac{\partial^2 W}{\partial Y^2}+\frac{\partial^2 W}{\partial Z^2}) \tag{4}$$

$$\frac{\partial \theta}{\partial \tau}+\frac{\partial}{\partial X}(U\theta)+\frac{\partial}{\partial Y}(V\theta)+\frac{\partial}{\partial Z}(W\theta)=(\frac{\partial^2 \theta}{\partial X^2}+\frac{\partial^2 \theta}{\partial Y^2}+\frac{\partial^2 \theta}{\partial Z^2}) \tag{5}$$

Where U, V and W are the velocity components in the X, Y and Z directions, respectively, P is the pressure, τ is thetime and θ the temperature. The non-dimensional variables used in these equations are defined by:

$$(X,Y,Z)=(\frac{x}{H},\frac{y}{H},\frac{z}{H}),(U,V,W)=(\frac{uH}{\alpha},\frac{vH}{\alpha},\frac{wH}{\alpha}),P=\frac{H^2}{\alpha^2}p,\tau=\frac{\alpha}{H^2}t \text{ and } \theta=\frac{T-T_C}{q''H}k \tag{6}$$

Where α, v and k represent respectively the thermal diffusivity, the kinematic viscosity and the thermal conductivity of the fluid.

In the above equations, the parameters Pr and Ra denote the Prandtl number, and the Rayleigh number, respectively. These parameters are defined by :

$$\Pr=\frac{\upsilon}{\alpha} \text{ and } \mathrm{Ra}=\frac{g\beta q''H^4}{\alpha\upsilon k} \tag{7}$$

The hydrodynamic boundary conditions are such as the velocity components are zero on the rigid walls of the enclosure ($U=V=W=0$). The dimensionless thermal boundary conditions associated to the governing equations are:

- Left vertical wall: $\frac{\partial \theta}{\partial X}=-1$ through the hot sections and $\frac{\partial \theta}{\partial X}=0$ elsewhere on the wall
- Right vertical wall: $\theta_c=0$ at $X=1$

- Other vertical and horizontal walls: $\dfrac{\partial \theta}{\partial n} = 0$ (n is the normal direction to the considered wall).

The local Nusselt number and the total average Nusselt number are respectively defined by:

$$\mathrm{Nu}(y,z) = \frac{q'' H}{(T(x,y)\,|_{x=0} - T_c)k} = \frac{1}{\theta(Y,Z)\,|_{X=0}} \tag{8}$$

$$\mathrm{Nu} = 2 \iint \mathrm{Nu}(y,z)\,dydz \tag{9}$$

Where $\theta(Y,Z)$, in equation (8), is the local dimensionless temperature at a given point of the heat source surface.

3 Numerical method

The governing equations (Navier-Stokes and energy equations) are discretized by the finite volume method adopting the power low scheme. The Alternating Direction Implicit scheme (ADI) is then used for solving the obtained algebric system. The tri-diagonal system obtained in each direction is solved using the THOMAS algorithm. Convergence of the numerical code is established at each time step according to the following criterion:

$$\sum_{i,j,k=1}^{i\max,j\max,k\max} \frac{\left|\phi_{i,j,k}^{n+1} - \phi_{i,j,k}^{n}\right|}{\left|\phi_{i,j,k}^{n}\right|} \leq 10^{-4} \tag{10}$$

Where ϕ is one of the field variables (U,V,W,T,P) and i, j and k the grid positions. n represents the time step number.

A study of the grid effect on the fluid flow and heat transfer was conducted for different sets of the governing parameters. Finally, the non-uniform staggered grid of $41 \times 41 \times 41$ nodes was estimated to be appropriate for the present study since it permits a good compromise between the computational cost (a significant reduction of the execution time) and the accuracy of the obtained results. The optimal time step was also found to be equal to 10^{-3} after multiple tests.

Thereafter, the code has been validated by comparing its results with those published by previous studies in the case of natural convection in a differentially heated cubical cavity. The tests were conducted by comparing with the results of Frederick and Quiroz (2001) and Ben-Cheikh, Campo, Ouertatani and Lili (2010) with a heating section of dimension $\varepsilon = 0.5$ placed on the vertical wall of the cavity. A

comparison of the maximum values of the velocities U and V in the plane $Z = 0.5$ is given in Table.1 for $Ra = 10^6$. The results are found to be in excellent agreement with the two references. Hence, the current solution differs by no more than 1.37% for $U_{\max}$ and 2.35% for $V_{\max}$ compared to Frederick and Quiroz (2001) and about 1.27% for $U_{\max}$ and 1.47% for $V_{\max}$ compared to Ben Cheikh et al. (2010).

Table 1: Validation of the numerical code with published results in terms $U_{\max}$ and $V_{\max}$ for $Z = 0.5$ and Ra $= 10^6$

Frederick and Quiroz (2001)		Ben-Cheikh, Campo, Ouertatani and Lili (2010)		Present work	
$U_{\max}$	$V_{\max}$	$U_{\max}$	$V_{\max}$	$U_{\max}$	$V_{\max}$
35.9146	63.2177	35.9436	65.6693	36.4020	64.7033

4 Results and discussions

The results presented in this section were obtained for Rayleigh numbers Ra ranging between 10^3 and 10^7 and the heating sections dimension ε between 0.15 and 0.35. The Prandtl number Pr and the aspect ratio $Ax = H/L$ are respectively fixed at 0.71 and 1.

4.1 Isotherms and streamlines

In order to visualize the flow and the temperature distribution within the studied configuration, streamlines and isotherms in 3D as well as isotherms on the heating sections are respectively shown in figures 2a and 2c, for $\varepsilon = 0.35$ and Ra $= 10^6$. It is seen that the fluid flow consists of a big and unique cell occupying the entire cavity. The fluid motion leads the heat from the active sections through the cavity. High values of the temperature are normally observed in the upper part of the enclosure. This trend is also encountered in the isotherms presented over the heating sections, as shown in figure 2c.

A presentation of isotherms and streamlines for different plans ($0 \leq Z \leq 1$) shows a good symmetry with respect to the plane $Z = 0.5$, due to the adopted geometry and thermal boundary conditions as shown in Fig. 3 in the case of $\varepsilon = 0.35$. Hence, for all the considered values of ε, the plane $Z = (2-\varepsilon)/6$, perpendicular to the middle of the section 1 and characterized by high thermal activity, is considered as a representative plan of the fluid motion and the heat transfer and is used for the following presentations. In addition, streamlines and isotherms in this plan presents a perfect symmetry relative to the plane $Z = 0.5$ and are therefore identical to those obtained in the plane $Z = (4+\varepsilon)/6$ perpendicular to the middle of the section 2.

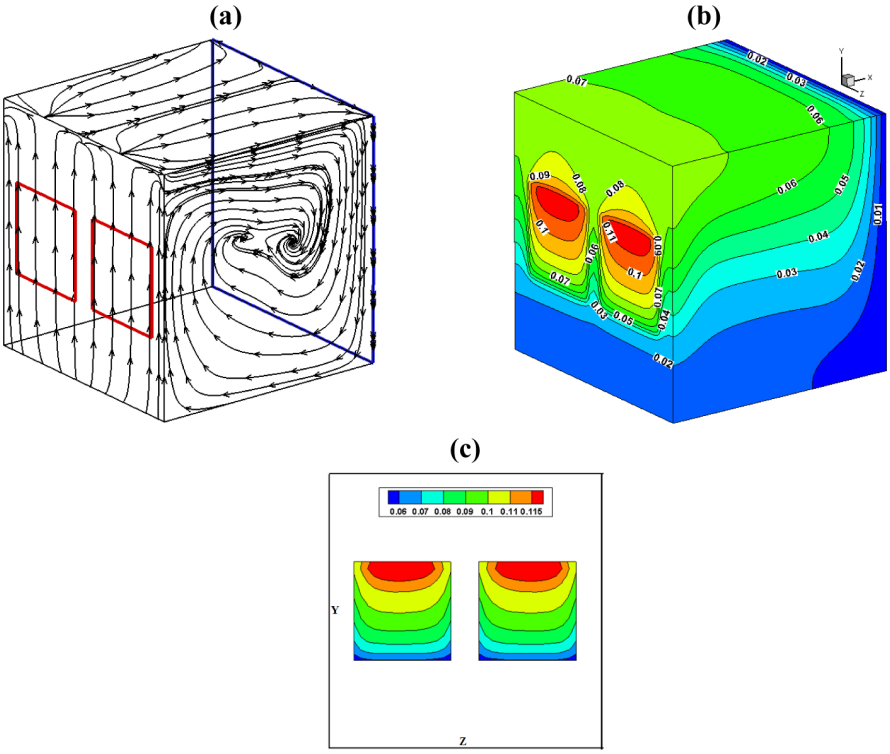

Figure 2: Streamlines 3D (a), isotherms 3D (b) and isotherms on the sections (c) for Ra $= 10^6$ and $\varepsilon = 0.35$

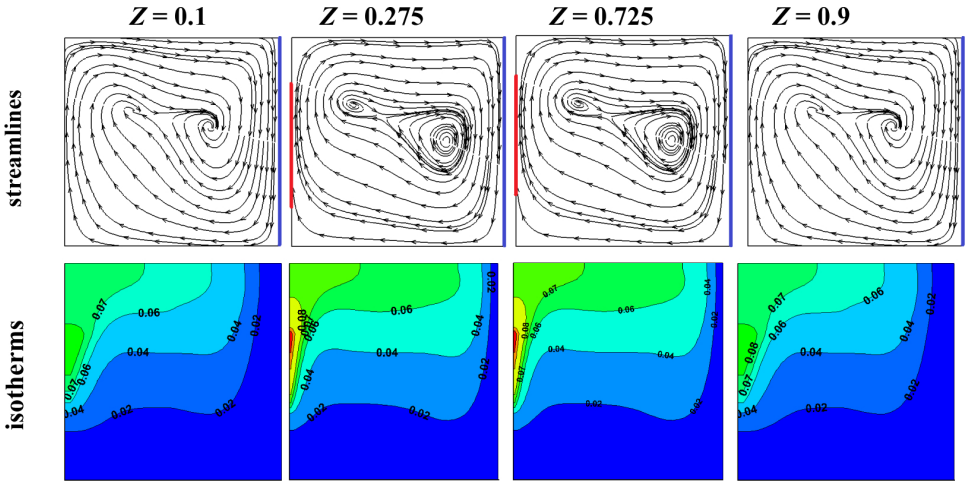

Figure 3: Streamlines, isotherms for different plans Z for $\varepsilon = 0.35$ and Ra $= 10^6$.

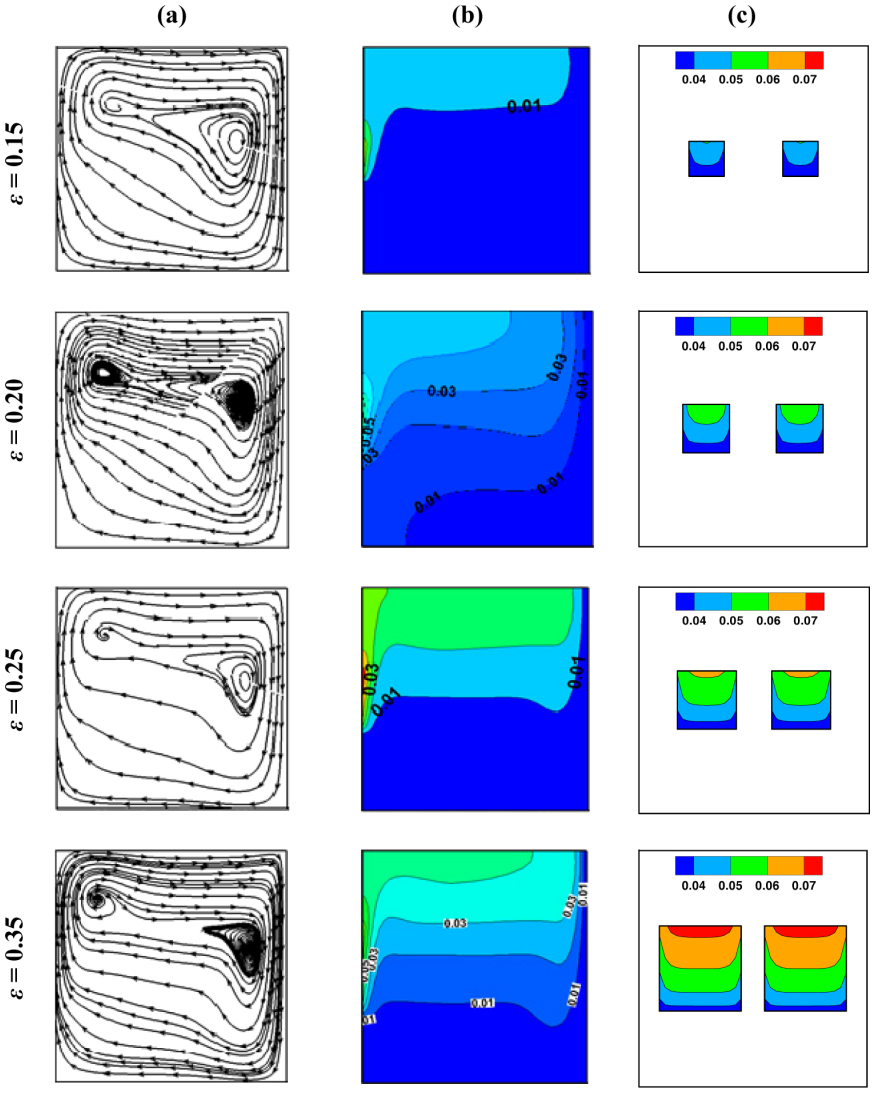

Figure 4: Streamlines (a) and isotherms (b) in the plane $Z = (2-\varepsilon)/6$ and isotherms on the sections (c) for $\mathrm{Ra} = 10^7$ and $0.15 \leq \varepsilon \leq 0.35$

In order to highlight the effect of the heating sections dimensions ε ($0.15 \leq \varepsilon \leq 0.35$), the hydrodynamic and thermal fields in the cavity are shown in fig. 4 for $\mathrm{Ra} = 10^7$ and different dimensions $\varepsilon = 0.15$, $\varepsilon = 0.20$, $\varepsilon = 0.25$ and $\varepsilon = 0.35$. For the four cases, figures 4a and 4b present respectively the streamlines and the isotherms in the plane $(2-\varepsilon)/6$ perpendicular to the middle of the section 1. Figures 4c present the isotherms over the two heating sections. For all the considered

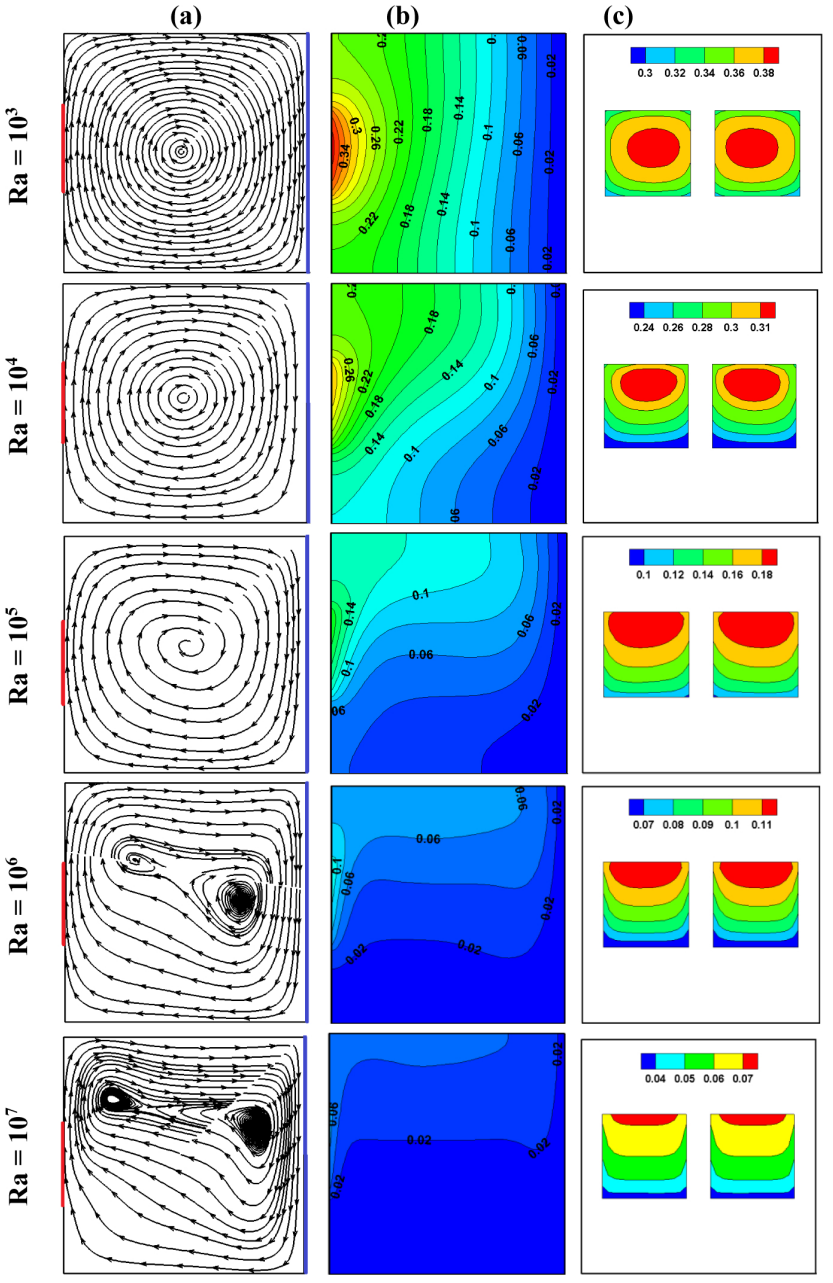

Figure 5: Streamlines (a) isotherms (b) obtained in the plane $Z = 0.275$ and isotherms at sections (c) for $\varepsilon = 0.35$ and $10^3 \leq \mathrm{Ra} \leq 10^7$

cases, the flow consists of a unique cell with cores intensity depending on the sections dimension. In addition, the temperatures at sections increase passing from the value $\theta_{max} = 0.0505$ for $\varepsilon = 0.15$ to the value $\theta_{max} = 0.0733$ for $\varepsilon = 0.35$. These maximum values are reached at the midpoints of the upper edges of the sections.

Figure 5 presents the effect of the Rayleigh number ($10^3 \leq Ra \leq 10^7$) on hydrodynamic and thermal fields for $\varepsilon = 0.35$. Streamlines and isotherms, shown by figures 5a and 5b respectively, are presented in the plane $Z = 0.275$, while figure 5c presents the isotherms over the two heating sections. For Rayleigh number Ra ranging between 10^3 and 10^4, the figure 5a shows that the flow consists of a single cell occupying the whole of the cavity, rotating in the clockwise direction, to evacuate the heat from the heating sections to the right cold vertical wall of the cavity. The core of the cell is located in the center of the cavity. The viscous forces are then more dominant than the buoyancy ones and diffusion remains the most important mode of heat transfer. The corresponding isotherms show the same trend (figure 5b). Temperatures on the heating sections are very high and maximum temperatures are located near the centers of these sections (figure 5c). For higher values of Ra (10^6 and 10^7), convection becomes the dominant mode of heat transfer. The cell cores moved to the active walls (figure 5a) involving very important heat exchange as shown in the isotherms figures (figure 5b). The maximum temperatures positions on the sections are moved upwards (figure 5c). Note that for all studied Rayleigh number Ra, the maximum temperatures are identical for the two heating sections ($\theta_{max\,1} = \theta_{max\,2}$).

4.2 Nusselt number

Figure 6 represents the total average Nusselt number, calculated at the two heating sections for Ra ranging between 10^3 and 10^7 and different values of ε ($0.15 \leq \varepsilon \leq 0.35$). Note that the average Nusselt numbers, calculated for all the considered cases, are found to be identical for the two heating section. As expected, the total average Nusselt number increases with the Rayleigh number and especially when Ra reaches the value 10^4. In addition, figure 6 shows that for fixed Rayleigh number, the average Nusselt number decreases with increasing ε. For example, for $Ra = 10^6$ and $\varepsilon = 0.15$, the average Nusselt number is 9.75%, 17.42% and 29.38% higher than the values corresponding to $\varepsilon = 0.20$, $\varepsilon = 0.25$ and $\varepsilon = 0.35$ respectively. This trend was also encountered in previous works of Sharif and Mohammad (2005) and Ben Cheikh, Ben Beya and Lili (2007 ref$_1$). Values of the total average Nusselt number, Nu, maximum temperatures over each component, $\theta_{max\,1}$ and $\theta_{max\,2}$ and their location (Y,Z) are reported in Table 2 and 3 for all the studied cases. These tables show that the maximum temperatures are always identical for the two sections and increases with increasing ε. Their locations on the sections

also vary slightly with changing ε.

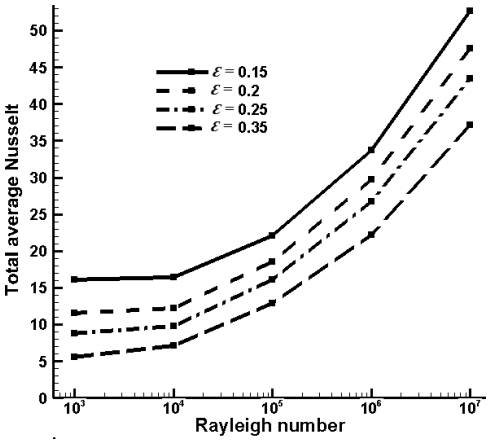

Figure 6: Variation of the total average Nusselt number with Rayleigh number for $0.15 \leq \varepsilon \leq 0.35$.

Table 2: Total average Nusselt number, *Nu* and maximum temperatures, $\theta_{\max 1}$ and $\theta_{\max 2}$ and their location (Y,Z) on the heated surfaces $\varepsilon = 0.15$ and 0.2

Rayleigh number, Ra	Dimensionless heat source length, ε	
	0.15	0.2
10^3	Nu = 16.15714	11.56593
	$\theta_{\max 1} = 0.1387$	0.1923 (0.5000,0.2949)
	$(Y,Z) = (0.5000,0.2949)$	0.1923 (0.5000,0.7051)
	$\theta_{\max 2} = 0.1387$	
	$(Y,Z) = (0.5000,0.7051)$	
10^4	16.40754	12.25177
	0.1368 (0.5000,0.2949)	0.1835 (0.5256,0.2949)
	0.1368 (0.5000,0.7051)	0.1835 (0.5256,0.7051)
10^5	22.12066	18.51133
	0.1068 (0.5256,0.2949)	0.1309 (0.5513,0.2949)
	0.1068 (0.5256,0.7051)	0.1309 (0.5513,0.7051)
10^6	33.71120	29.70371
	0.0757 (0.5513,0.2949)	0.0878 (0.5769,0.2949)
	0.0757 (0.5513,0.7051)	0.0878 (0.5769,0.7051)
10^7	52.64849	47.51788
	0.0505 (0.5769,0.2949)	0.0563 (0. 6026,0.2949)
	0.0505 (0.5769,0.7051)	0.0563 (0. 6026,0.7051)

Table 3: Total average Nusselt number, *Nu* and maximum temperatures, $\theta_{\max 1}$ and $\theta_{\max 2}$ and their location (Y,Z) on the heated surfaces $\varepsilon = 0.25$ and 0.35

Rayleigh number, Ra	**Dimensionless heat source length, ε** 0.25	0.35
10^3	Nu = 8.736535	5.563587
	$\theta_{\max 1} = 0.2524$	0. 3892 (0.5256,0.2949)
	$(Y,Z) = (0.5000,0.2949)$	0. 3892 (0.5256,0.7051)
	$\theta_{\max 2} = 0.2524$	
	$(Y,Z) = (0.5000,0.7051)$	
10^4	9.829109	7.162944
	0.2296 (0.5513,0.2949)	0. 3201 (0.6026,0.2692)
	0.2296 (0.5513,0.7051)	0. 3201 (0.6026,0.7308)
10^5	16.12001	12.87356
	0.1533 (0.5769, 0.2949)	0. 1971 (0.6282,0.2436)
	0.1533 (0.5769, 0.7051)	0. 1971 (0.6282,0.7564)
10^6	26.70839	22.23456
	0.0987 (0.6026,0.2949)	0. 1199 (0.6538,0.2436)
	0.0987 (0.6026,0.7051)	0. 1199 (0.6538,0.7564)
10^7	43.47707	37.18048
	0.0618 (0.6282,0.2949)	0. 0733 (0.6795,0.2692)
	0.0618 (0.6282,0.7051)	0. 0733 (0.6795,0.7308)

5 Conclusion

Three dimensional natural convection in a cavity discretely heated from the side has been studied for different sets of the governing parameters (Rayleigh number and heating sections dimensions) and leads to the following conclusions:

- The fluid flow consists of a big cell occupying the entire cavity for all the considered cases ($10^3 \leq \mathrm{Ra} \leq 10^7$) and ($0.15 \leq \varepsilon \leq 0.35$);
- The total average heat transfer, calculated in the two heating sections, increases with the Rayleigh number Ra and very significantly beyond $Ra = 10^4$;
- For fixed Rayleigh number, the average Nusselt number decreases with increasing ε.

References

Belarche, L.; Abourida, B.; Smolen, S.; Mediouni, T. (2014): Effect of the inclination on three-dimensional Incompressible fluid flowin a discretely heated cavity, *Key Engineering Materials*, vol. 597, pp 3-8.

Belarche, L.; Abourida, B.; Mediouni, T.; Mir, A. (2013): Étude tridimensionnelle de l'effet de la dimension des sections chauffantes au sein d'une cavité inclinée, *Revue Internationale d'Héliotechnique Energie-Environnement,* vol. 45, pp. 37-44.

Bejan, A.; Kraus, A. D.(2003): *Heat Transfer Handbook*. Wiley. New York.

Ben Cheikh, N.; Ben Beya, B.; Lili, T. (2007ref$_1$): Influence of thermal boundary conditions on natural convection in a square enclosure partially heated from below, *Int. J. Heat and Mass Transfer.*, vol. 34, pp. 369–379.

Ben Cheikh, N.; Ben Beya, B. ; Lili, T. (2007ref$_2$) : Étude thermique du refroidissement d'un ou plusieurs composants électroniques, *13èmes Journées Internationales de Thermique*, Albi, France.

Ben-Cheikh, N.; Campo, A.; Ouertatani, N.; Lili T. (2010): Three-dimensional study of heat and fluid flow of air and dielectric liquids filling containers partially heated from below and entirely cooled from above, *Int. J. Heat Transfer*., vol. 37, pp. 449–456.

Frederick, R.L.; Quiroz, F. (2001): On the transition from conduction to convection regime in a cubical enclosure with a partially heated wall, *Int. J. Heat Transfer*. vol. 44, pp. 1699–1709.

Fusegi, T.; Hyun, J.M.; Kuwahara K.; Farouk B. (1991): A numerical study of three-dimensional natural-convection in a differentially heated cubical enclosure, *Int. J. Heat Mass Transfer*. vol. 34, pp. 1543-1557.

Goldstein, R.J.; Ibele, W.E.; Patankar, S.V.; Simon, T.W.; Kuehn, T.H.; Strykowski, P.J.; Tamma, K.K.; Heberlein, J.V.R.; Davidson, J.H.; Bischof, J.; Kulacki, F.A.; Kortshagen, U.; Garrick, S.; Srinivasan, V. (2006): A review of 2003 literature. *Int. J. of Heat and Mass Transfer*.,vol. 49, pp. 451-534.

Patankar, S.V. (1980): *Numerical Heat Transfer and Fluid Flow.* McGraw-Hill. New York.

Seza, I.; Mohamad, A. A. (2000): Natural convection from a discrete heat source on the bottom of a horizontal enclosure, *Int. J. of Heat and Mass Transfer*, vol. 43, pp. 2257-2266.

Sharif, M.A.R.; Mohammad, T.R. (2005): Natural convection in cavities with constant flux heating at the bottom wall and isothermal cooling from the sidewalls, *Int. J. Therm. Sci.,* vol. 44, pp.865–878.